Journal of Sound and Vibration (2000) **229**(1), 113–132
Article No. jsvi.1999.2480, available online at http://www.idealibrary.com on IDEAL®

BOUNDARY CONTROL FOR A GENERAL CLASS OF NON-LINEAR STRING–ACTUATOR SYSTEMS

F. ZHANG, D. M. DAWSON AND S. P. NAGARKATTI

Department of Electrical and Computer Engineering, Clemson University, Clemson, SC 29634-0921, *U.S.A.*

AND

C. D. RAHN

Department of Mechanical Engineering, Clemson University, Clemson, SC 29634-0921, *U.S.A.*

(*Received* 25 *September* 1998, *and in final form* 18 *June* 1999)

This paper introduces boundary controllers for a general class of non-linear string–actuator systems. The non-linear distributed-parameter model accounts for large amplitude displacement and the associated varying tension according to a general class of non-linear stress–strain relationships. A non-linear, model-based controller asymptotically drives the system energy to zero. Redesign of the controller using adaptation laws allows compensation for parametric uncertainty while asymptotically driving the system energy to zero. Experimental results verify the feasibility of implementing the proposed controllers and compare the performance with damper and linear controllers.

1. INTRODUCTION

Many flexible mechanical systems exhibit vibration in the presence of disturbances. Often a cost-effective and practical method for reducing vibration is to actively apply control forces through actuators located at the boundary of the mechanical system. Several researchers [1–4] have proposed boundary controllers for a variety of flexible systems. With regard to some of the recent boundary control work for string-like systems, Baicu *et al.* [5] propose a linear, stabilizing boundary controller for a flexible cable system that utilizes the cable "slope" at the actuated boundary as a feedback signal. In reference [6], Morgül designs boundary feedback controllers for the wave equation that include proportional and strictly positive real derivative feedback. Shahruz *et al.* [7] illustrate how a standard boundary damper can be used to exponentially stabilize a string model that includes non-linear tension effects. Canbolat *et al.* [8] use measurements of the slope, slope-rate, and the velocity at the cable's actuated boundary to develop an exponentially stabilizing boundary controller for the cable model used in reference [5]. Recently, researchers

0022-460X/00/010113 + 20 $35.00/0

have illustrated how boundary controllers previously designed for string-like models can be used to control vibration in axially moving material systems (e.g., web-handling systems). For example, Quieroz *et al.* [9] design an interstitial controller that regulates the displacement of an axially moving string by applying a control force and a control torque to the web via a mechanical guide. Shahruz [10] illustrates how a standard boundary damper can be used to stabilize an axially moving string model that includes non-linear tension effects.

In this paper, we relax several important assumptions in the previous research to enlarge the applicability of boundary control for string systems. Specifically, the model used for control design purposes includes non-linear terms in the field equation and actuator boundary condition resulting from large amplitude displacements and non-linear elastic effects. This model reduces to that used in reference [7] if the mass of the actuator is equal to zero and the slope of the displacement is sufficiently small. Based on the proposed model for the string–actuator system, we design a model-based boundary controller that asymptotically drives the total energy of the string–actuator system to zero. The proposed boundary controller is a non-linear algorithm that requires measurement of: (1) the string's slope (and its time derivative) at the actuated boundary, (2) the string's velocity at the actuated boundary, and (3) the tension in the string. We then redesign the model-based boundary controller as an adaptive boundary controller that compensates for parametric uncertainty and asymptotically drives the total energy of the system to zero. The performance of the controller is demonstrated via experimental results.

2. DYNAMIC MODEL

As in reference [11], we neglect the tangential and out-of-plane displacement of the string–actuator system of Figure 1 and assume

$$T(t) \ll EA, \tag{1}$$

where E denotes the string Young's modulus, A represents the string cross-sectional area, and $T(t)$ is the time-varying string tension. This assumption implies that the tension is uniform along the string (i.e., independent of x). We assume that the tension function has the following properties: (1) $T(y(t))$ is a strictly positive function that satisfies

$$T(y(t)) \geqslant T_0 > 0, \tag{2}$$

where $y(t)$ is the string stretch, (2) if $y(t)$ is bounded, $T(y(t))$ is also bounded, and (3) the potential energy stored in the string can be lower and upper bounded as follows:

$$\alpha_l y(t) \leqslant PE = \int_0^y T(y(t))\,\mathrm{d}y \leqslant \kappa_u(y(t)), \tag{3}$$

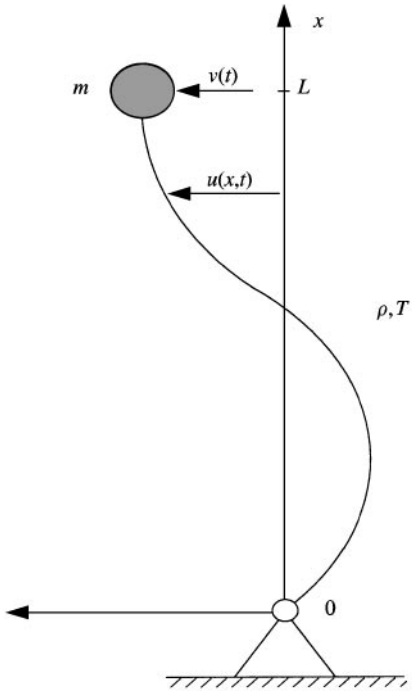

Figure 1. Schematic diagram of the string–actuator model.

where α_l is a positive scalar constant, $\kappa_u(\cdot)$ is some continuous class K function.† The string stretch is given by

$$y(t) = \int_0^L (-1 + \sqrt{1 + (u_x(x,t))^2}), \mathrm{d}x > 0, \tag{4}$$

where L denotes the string length, $x \in [0, L]$ denotes the independent position variable, t denotes the independent time variable, $u(x, t)$ denotes the transverse displacement at position x for time t, and the subscripts x and t denote the partial derivatives with respect to x and t respectively.

As in reference [12], the transverse dynamics for the mechanical system depicted in Figure 1 are of the form

$$\rho u_{tt}(x,t) = [T(y(t)) \sin(\theta(x,t))]_x, \tag{5}$$

where ρ denotes the mass per unit length of the string, and $\theta(x, t)$ denotes the angular inclination of the string tangent with respect to x axis. It can be shown [12] that

$$\sin(\theta(x,t)) = \frac{u_x(x,t)}{\sqrt{1 + (u_x(x,t))^2}}. \tag{6}$$

†A continuous function $\kappa(p)$ is said to be class K if: (i) $\kappa(0) = 0$, (ii) $\kappa(p) > 0\ \forall p > 0$, and (iii) $\kappa(p)$ is non-decreasing.

As illustrated in Figure 1, one boundary of the string is pinned, and the other boundary is connected to an actuator. Since we have assumed that the tension is uniform along the string, we can now use equations (6) and (5) to formulate the non-linear partial differential equation (PDE) and boundary conditions[‡] for the string–actuator system as follows:

$$\rho u_{tt}(x, t) = T(y(t))\left[\frac{u_x(x, t)}{\sqrt{1 + (u_x(x, t))^2}}\right]_x \quad \text{for } x \in (0, L), \tag{7}$$

$$u(0, t) = 0, \tag{8}$$

$$m u_{tt}(L, t) + T(y(t))\frac{u_x(L, t)}{\sqrt{1 + (u_x(L, t))^2}} + Y(u_t(L, t))\phi = v(t), \tag{9}$$

where m denotes the mass of the actuator at the boundary $x = L$, $v(t)$ denotes the control input force at the boundary, and the term $Y(u_t(L, t))\phi$ is a linear parameterization representing additional actuator dynamics (e.g., friction) with $Y(\cdot) \in \Re^{1\times p}$ a regression matrix and $\phi \in \Re^p$ a parameter vector.

Remark 1. It can be shown that the dynamics given by equations (7)–(9) reduce to the linear string model if a linear stress–strain relationship is used:

$$T(y(t)) = T_0 + \frac{EA}{L}y(t), \tag{10}$$

and the slope of the transverse displacement is small (i.e., $u_x(x, t) \ll 1$ allows $\sqrt{1 + (u_x(L, t))^2}$ to be replaced by unity in equations (7), (9), and (4)). Note that the model used in reference [7] can also be obtained from equations (7)–(9) under the assumptions: (1) the mass at the actuator is equal to zero (i.e., $m = 0$), (2) the string tension is given in equation (10), (3) the slope of the transverse displacement is small (i.e., $u_x(x, t) \ll 1$ allows $\sqrt{1 + (u_x(L, t))^2}$ to be replaced by unity in equations (7) and (9)), and (4) using $1 + \frac{1}{2}(u_x(x, t))^2$, as opposed to unity, as a better than linear approximation for $\sqrt{1 + (u_x(x, t))^2}$ in equation (4). The $T(y(t))$ of equation (10) is strictly positive and satisfies equation (3) for some α_l and $\kappa_u(\cdot)$; furthermore, most stress–strain models (e.g., polynomial) satisfy the mild assumptions imposed by equations (2) and (3).

Remark 2. Note that if the control input $v(t)$ equals zero, then the system given by equations (7) and (9) is conservative (i.e., $KE + PE = \text{constant}$).

3. CONTROL FORMULATION

3.1. MODEL-BASED CONTROL LAW

The primary control objective is to design an asymptotically regulating controller for the dynamics of equations (7)–(9). Based on the subsequent stability

[‡] The pinned boundary condition (8) implies that $u_t(0, t) = 0$.

analysis, we propose the following non-linear, boundary controller:

$$v(t) = -\frac{mu_{xt}(L,t)}{(1+(u_x(L,t))^2)^{3/2}} + T(y(t))\frac{u_x(L,t)}{\sqrt{1+(u_x(L,t))^2}} + Y(u_t(L,t))\phi - \left(k + \frac{k_r}{2}T(y(t))\right)\eta(t), \tag{11}$$

where

$$\eta(t) = u_t(L,t) + \frac{u_x(L,t)}{\sqrt{1+(u_x(L,t))^2}} \tag{12}$$

and k, k_r are scalar control gains chosen to satisfy

$$k > 0 \quad \text{and} \quad k_r \geqslant 1. \tag{13}$$

Remark 3. Equations (11) and (12) show that the controller requires measurement of $u_{xt}(L,t)$, $u_x(L,t)$, $u_t(L,t)$ and $T(y(t))$. These quantities can be measured at the actuated boundary using standard sensors. Specifically, $T(y(t))$ can be measured by a load cell, $u_x(L,t)$ can be measured by a load cell or an encoder, and $u(L,t)$ can be measured by an encoder. The quantities $u_{xt}(L,t)$ and $u_t(L,t)$ can be approximated numerically by differentiating $u_x(L,t)$ and $u(L,t)$ with respect to time, respectively.

After differentiation of equation (12) with respect to time, multiplication of both sides by m, and substitution for $mu_{tt}(L,t)$ from the boundary condition (9), we obtain the following open-loop dynamics for $\eta(t)$:

$$m\dot{\eta}(t) = \frac{mu_{xt}(L,t)}{(1+(u_x(L,t))^2)^{3/2}} - T(y(t))\frac{u_x(L,t)}{\sqrt{1+(u_x(L,t))^2}} - Y(u_t(L,t))\phi + v(t), \tag{14}$$

where $\dot{\eta}(t) = (\mathrm{d}/\mathrm{d}t)(\eta(t))$. After substitution of the control input (11) in the right-hand side of equation (14), we obtain the closed-loop dynamics for $\eta(t)$,

$$m\dot{\eta}(t) = -\left(k + \frac{k_r}{2}T(y(t))\right)\eta(t). \tag{15}$$

Theorem 1. *Given the field equation* (7), *boundary condition* (8), *and closed-loop boundary condition* (15), *kinetic energy* (18) *and potential energy* (3) *of the string–actuator system decay asymptotically to zero.*

Proof. We first prove that all signals in the closed-loop system are bounded. We define the following non-negative, scalar function

$$V_1(t) = E(t) + \tfrac{1}{2}m\eta^2(t), \tag{16}$$

where

$$E(t) = \frac{1}{2}\int_0^L \rho u_t^2(x,t)\,\mathrm{d}x + \int_0^y T(y(t))\,\mathrm{d}y. \tag{17}$$

From the structure of $V_1(t)$ given by equations (16) and (17), we can see that $V_1(t) \geqslant 0$. In Lemma 1 (Appendix A) we show that $\dot{V}_1(t) \leqslant 0$; hence, since $\dot{V}_1(t)$ is bounded below by zero and is decreasing or constant, we know that $V_1(t)$ is bounded ($V_1(t) \in L_\infty$). Since $V_1(t) \in L_\infty$, we can see from equation (16) that $E(t)$ of equation (17) and $\eta(t)$ of equation (12) are also bounded for all time. Since $E(t) \in L_\infty$, it follows that the potential energy of the system defined in equation (3) is bounded.

Remark 4. Since the proposed control strategies are relatively simple, smooth functions, we will assume the existence of a solution for the dynamics given above under the proposed control. To illustrate that the control force is bounded, we will invoke the assumptions that the displacement $u(x, t)$ and its time derivative $u_t(x, t)$ belong to a space of functions that has the following properties: (1) if the potential energy of system (3) is bounded, then $u(x, t)$, $u_x(x, t)$, and $u_{xx}(x, t)$ are bounded for all $(x, t) \in [0, L] \times [0, \infty)$, and (2) if the kinetic energy of the system is bounded then $u_t(x, t)$ and $u_{xt}(x, t)$ are bounded for all $(x, t) \in [0, \mathrm{L}] \times [0, \infty)$ where the kinetic energy of the system is given by

$$KE = \frac{1}{2}\left(\int_0^L \rho u_t^2(x, t)\,\mathrm{d}x + m u_t^2(L, t)\right). \tag{18}$$

These assumptions are reasonable because if the energy of a real physical system is bounded then all the signals that make up the governing dynamic equations should also remain bounded.

From the assumption in Remark 4, we assume that $u(x, t)$, $u_x(x, t)$, and $u_{xx}(x, t)$ are also bounded for all $(x, t) \in [0, L] \times [0, \infty)$. From the boundedness of $\eta(t)$, we use equation (12) to show that $u_t(L, t)$ is bounded. Since $E(t)$, $\eta(t) \in L_\infty$, the kinetic energy of the system given by equation (18) is bounded; hence, we can use Remark 4 to show that $u_t(x, t)$ and $u_{xt}(x, t)$ are bounded for all $(x, t) \in [0, L] \times [0, \infty)$. In addition, since the potential energy is bounded, it is easy to see from equation (3) that $y(t)$ defined in equation (4) is also bounded. Since $y(t) \in L_\infty$, we can use the properties of $T(y(t))$ of equation (2) to state that $T(y(t)) \in L_\infty$. Since $u_x(L, t)$, $u_t(L, t)$, $u_{xt}(L, t)$, $\eta(t)$, and $T(y(t)) \in L_\infty$, we know that the control force $v(t)$ given by equation (11) is bounded. Finally, since $\eta(t)$ and $T(y(t)) \in L_\infty$, we can use equation (15) to state that $\dot{\eta}(t) \in L_\infty$. From the above information, we can now use equations (7) and (9) to show that $u_{tt}(x, t)$ is bounded for all $(x, t) \in [0, L] \times [0, \infty)$.

To prove that the kinetic energy and the potential energy of the string–actuator system decay asymptotically to zero, we define the scalar function

$$V(t) = V_1(t) + E_c(t), \tag{19}$$

where $E_c(t)$ is defined as

$$E_c(t) = 2\beta\rho \int_0^L x u_t(x, t) u_x(x, t)\,\mathrm{d}x \tag{20}$$

and β is a positive weighting constant. In Lemma 2 (Appendix A), we show that the positive constant β can be selected small enough such that the function $V(t)$ of equation (19) can be bounded below and above in the following manner:

$$0 \leqslant \lambda_1(E_a(t) + \eta^2(t)) \leqslant V(t) \leqslant \lambda_2(E(t) + \eta^2(t)), \tag{21}$$

where λ_1, λ_2 are positive constants defined in Lemma 2 and

$$E_a(t) = \frac{1}{2}\int_0^L \rho u_t^2(x, t)\,\mathrm{d}x + y(t). \tag{22}$$

In Lemma 3 (Appendix A), we show that the positive constant β can be selected small enough such that the time derivative of the function $V(t)$ of equation (19) can be upper bounded as follows:

$$\dot{V}(t) \leqslant -\kappa_0\left(\int_0^L\left(-1 + \sqrt{1 + (u_x(x, t))^2}\right)\mathrm{d}x + \int_0^L u_t^2(x, t)\,\mathrm{d}x + u_t^2(L, t)\right) \triangleq -g(t), \tag{23}$$

where κ_0 is some positive constant and $g(t)$ is a non-negative, scalar function defined by equation (23). Since $u_x(x, t)$, $u_t(x, t)$, $u_{xt}(x, t)$, $u_{tt}(x, t)$, and $u_{xx}(x, t)$ are all bounded for all $(x, t) \in [0, L] \times [0, \infty)$, $\dot{g}(t) \in L_\infty$; hence, from equation (23), we can now invoke Lemma 4 (Appendix A) to show that

$$\lim_{t\to\infty} g(t) = 0. \tag{24}$$

From the structure of $g(t)$ defined in equation (23), we can use equations (24), (18), (3) and (4) to show that the kinetic energy and the potential energy of the system decay asymptotically to zero. □

Remark 5. Intuitively, if the total energy is driven to zero, one would expect that the transverse displacement for the string–actuator should also approach zero (i.e., $\lim_{t\to\infty} KE + PE = 0 \Rightarrow \lim_{t\to\infty} |u(x, t)| = 0$); however, for the non-linear string–actuator dynamics given by equations (7)–(9), there does not seem to be a straightforward way to use the result of Theorem 1 to prove $\lim_{t\to\infty} |u(x, t)| = 0$.

3.2. ADAPTIVE CONTROL LAW

In this subsection, we redesign the model-based controller of equation (11) to compensate for parametric uncertainty. We now rewrite the open-loop dynamics for $\eta(t)$ defined in equation (12) as follows:

$$m\dot{\eta}(t) = W(\cdot)\theta - T(y(t))\frac{u_x(L, t)}{\sqrt{1 + (u_x(L, t))^2}} + v(t), \tag{25}$$

where the matrix $W(u_{xt}(L, t), u_t(L, t)) \in \Re^{1\times(p+1)}$ is given by

$$W(\cdot) = \left[\frac{u_{xt}(L, t)}{(1 + (u_x(L, t))^2)^{3/2}}, \quad -Y(u_t(L, t))\right] \tag{26}$$

and the unknown parameter vector $\theta \in \Re^{p+1}$ is given by

$$\theta = [m, \phi^{\mathrm{T}}]^{\mathrm{T}}. \tag{27}$$

The adaptive controller consists of the control law

$$v(t) = -W(\cdot)\hat{\theta} + T(y(t))\frac{u_x(L,t)}{\sqrt{1+(u_x(L,t))^2}} - \left(k + \frac{k_r}{2}T(y(t))\right)\eta(t) \tag{28}$$

and the adaptation algorithm

$$\dot{\hat{\theta}}(t) = \Gamma W^{\mathrm{T}}(\cdot)\eta(t) \tag{29}$$

that calculates the parameter estimate $\hat{\theta}(t)$ on-line. The adaptation gain matrix $\Gamma \in \Re^{(p+1)\times(p+1)}$ is diagonal, positive-definite, and constant. After substituting equation (28) into equation (25), we obtain the closed-loop dynamics expression for $\eta(t)$ as

$$m\dot{\eta}(t) = -\left(k + \frac{k_r}{2}T(y(t))\right)\eta(t) + W(\cdot)\tilde{\theta}(t), \tag{30}$$

where $\tilde{\theta}(t) = \theta - \hat{\theta}(t) \in \Re^{p+1}$ denotes the parameter estimation error vector.

It can easily be shown that the adaptive controller of equations (28) and (29) ensures the same stability as that of Theorem 1. Specifically, to prove that all signals in the closed-loop system are bounded, we can utilize the non-negative function

$$V_{1a}(t) = V_1(t) + \tfrac{1}{2}\tilde{\theta}^{\mathrm{T}}(t)\Gamma^{-1}\tilde{\theta}(t), \tag{31}$$

where $V_1(t)$ was defined in equation (16). After differentiating $V_{1a}(t)$ with respect to time and substituting equations (30) and (29), we can show that $\dot{V}_{1a}(t) \leqslant 0$ in the same manner as Lemma 1. In a similar manner to that used in the proof of Theorem 1, we can show that all the signals in the closed-loop system and the controller are bounded for all time.

To prove that the kinetic energy and the potential energy of the string–actuator system defined by equations (18) and (3) decay asymptotically to zero, we utilize the function

$$V_a(t) = V(t) + \tfrac{1}{2}\tilde{\theta}^{\mathrm{T}}(t)\Gamma^{-1}\tilde{\theta}(t), \tag{32}$$

where $V(t)$ was defined in equation (19). Using a similar procedure as in Lemma 2, we can show that the function $V_a(t)$ equation of (32) can be lower and upper bounded in the following manner:

$$0 \leqslant \lambda_{1a}(E_a(t) + \eta^2(t) + \|\tilde{\theta}(t)\|^2) \leqslant V_a(t) \leqslant \lambda_{2a}(E(t) + \eta^2(t) + \|\tilde{\theta}(t)\|^2), \tag{33}$$

where λ_{1a}, λ_{2a} are positive constants. After following a process similar to that of Lemma 3, we obtain

$$\dot{V}_a(t) \leqslant -g(t), \tag{34}$$

where $g(t)$ was defined in equation (23). Hence, we can repeat the same stability arguments used in proof of Theorem 1 to show that the kinetic energy and the potential energy of the string–actuator system decay asymptotically to zero.

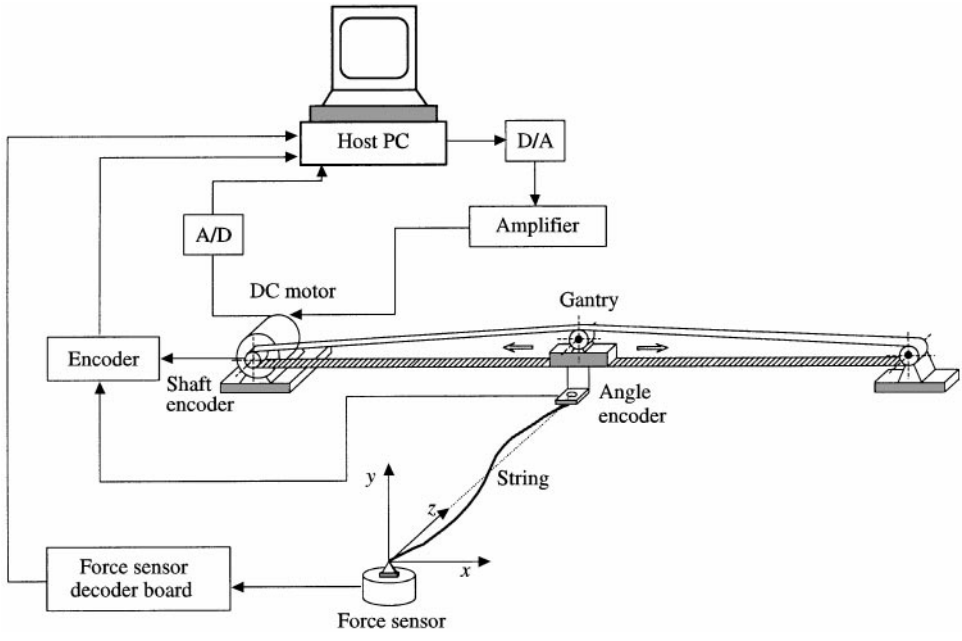

Figure 2. Schematic diagram of the experimental setup.

4. EXPERIMENTAL RESULTS

4.1. EXPERIMENTAL SETUP

Figure 2 shows a schematic diagram of the experimental setup used to implement the controllers. The setup consists of a flexible string pinned at one end and attached to a linearly translating gantry at the other end. A brushless DC motor (Baldor model 3300) drives the gantry via a belt-pulley transmission. The gantry rides on two parallel 1-in diameter steel rods on linear bearings. The displacement of the gantry, $u(L, t)$, is obtained from a 1000-count rotary encoder (Hohner) attached to the motor shaft. The static and dynamic tension measurement of the string, $T(t)$, is obtained from the JR3 force sensor attached to the string at the pinned end. A hollow-shaft 1000-count rotatory encoder is mounted on the gantry to measure the string deflection angle, $u_x(L, t)$, at the free end.

A Pentium 166 MHz PC running QNX (a real-time micro-kernel-based operating system) hosts the control algorithm. *Qmotor*, a graphical user-interface developed in-house, provides an environment to write the control algorithm in "C" programming language. It also provides features such as on-line graphing and allows the user to vary control gains without having to recompile the program. The *MultiQ* I/O board provides for data transfer between the computer subsystem and the electrical interface. An A/D channel measures the current flowing through the windings of the DC motor as sensed by a Hall-effect current sensor. One D/A channel drives the DC motor through a Techron linear power amplifier providing upto 10 A at 100 V. All the controllers are implemented using a sampling period of

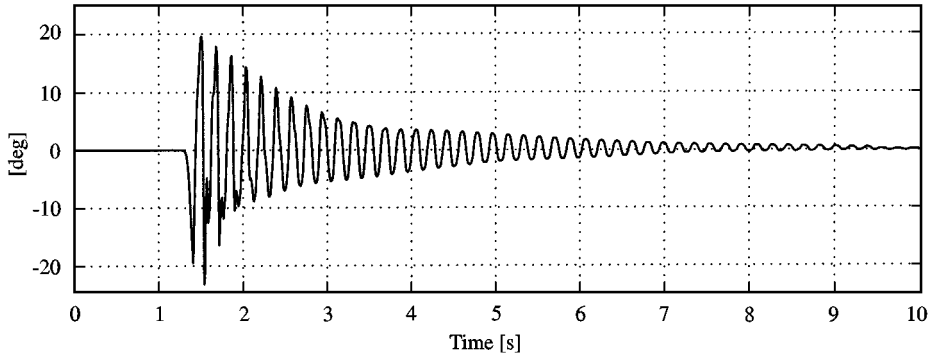

Figure 3. Experimental results in open-loop mode: string deflection angle $u_x(L, t)$.

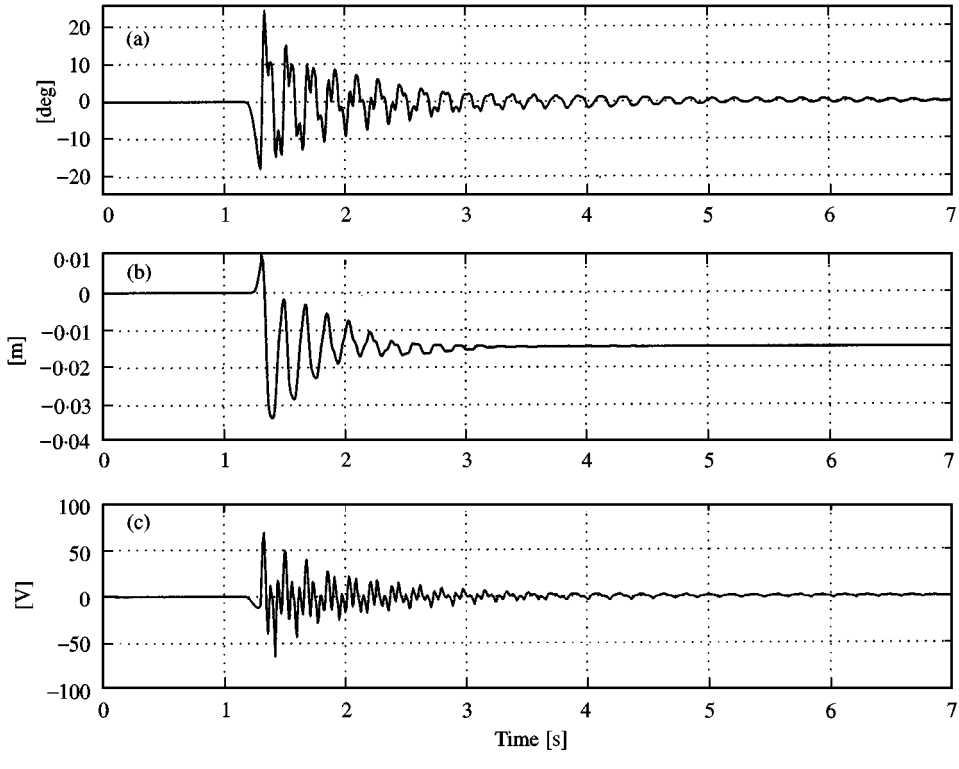

Figure 4. Experimental results for damper controller: (a) string deflection angle $u_x(L, t)$, (b) gantry displacement $u(L, t)$, and (c) control voltage.

0·5 m s. The velocity of the gantry and time derivative of the string deflection angle are obtained using a backwards difference algorithm applied to the gantry position and the string deflection angle, respectively, with the resulting signals filtered by a second order digital filter. Trapezoidal integration implements the adaptive update laws (29). The parameter values for the mechanical system are $m = 3{\cdot}5$ kg, $\rho = 0{\cdot}03$ kg/m, $L = 0{\cdot}31$ m.

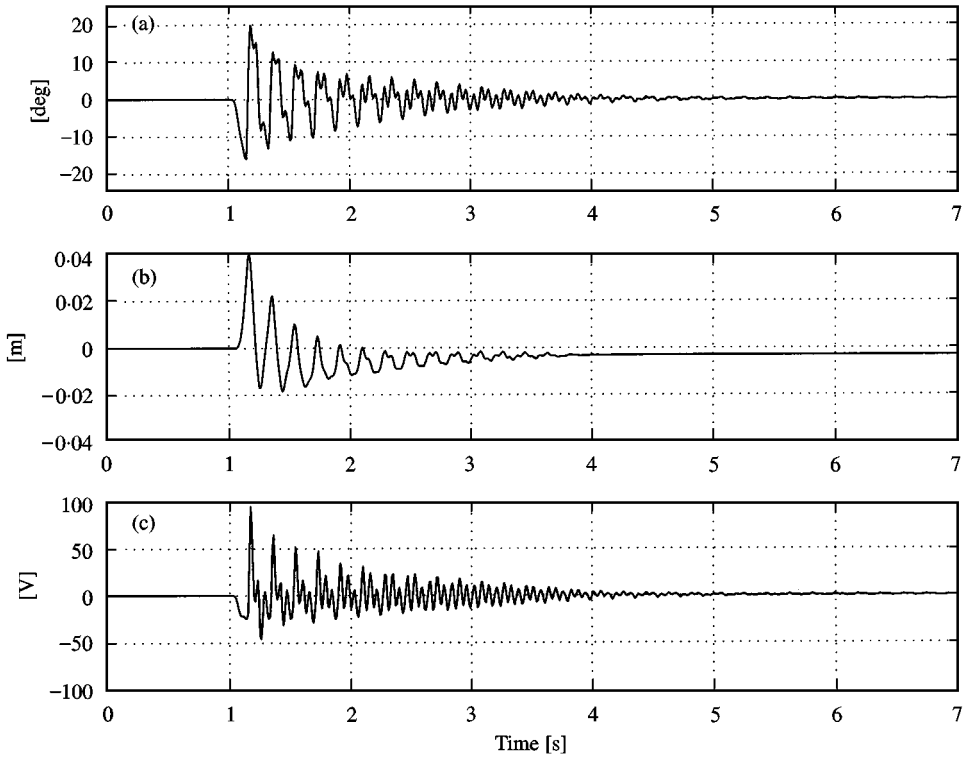

Figure 5. Experimental results for linear controller: (a) string deflection angle $u_x(L, t)$, (b) gantry displacement $u(L, t)$, and (c) control voltage.

4.2. EXPERIMENTAL RESULTS

Five experiments are conducted to assess the performance of the proposed controllers. The transient response to a consistent initial displacement is studied. The control gains are tuned to provide the best response.

Figure 3 shows the string response to the initial displacement without control (open loop, $v(t) = 0$). The response decays under natural damping in approximately 10 s. In Figure 4, a damper control law

$$v(t) = -k_d u_t(L, t) \tag{35}$$

decreases the settling time to approximately 7 s with $k_d = 4{\cdot}25$.

For small transverse displacement, the model-based controller of equation (11) becomes a *linear controller* as follows:

$$v(t) = -mu_{xt}(L, t) + T_0 u_x(L, t) - \left(k + \frac{k_r}{2} T_0\right)\eta(t), \tag{36}$$

where T_0 is the mean tension and the actuator compensation term $Y(u_t(L, t))\phi$ is not used. The linear control is implemented with $T_0 = 29{\cdot}75$ N and achieves the best regulation results with $k = 2{\cdot}6$ and $k_r = 3{\cdot}0$ shown in Figure 5. The inclusion of

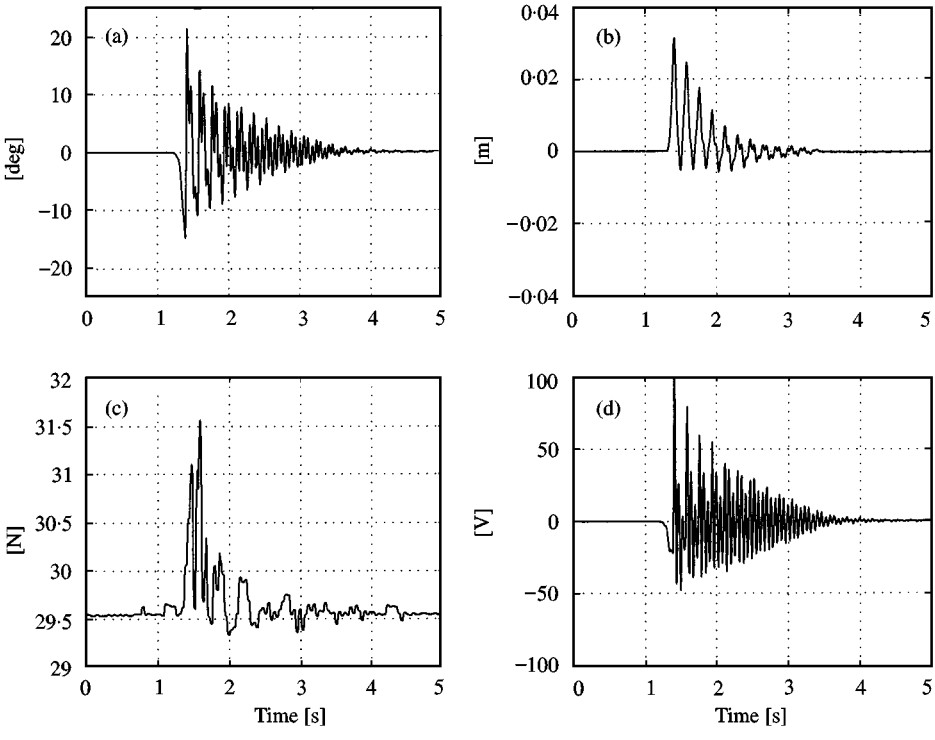

Figure 6. Experimental results for model-based controller: (a) string deflection angle $u_x(L, t)$, (b) gantry displacement $u(L, t)$, (c) tension $T(t)$, and (d) control voltage.

string slope feedback in the control causes more gantry motion and a corresponding increased damping, reducing the settling time to 6 s.

The fourth experiment uses the model-based control (11) with[§]

$$Y(\cdot) = [\text{sgn}(u_t(L, t)),\ u_t(L, t)], \qquad \phi = [F_s,\ F_d]^{\text{T}}, \tag{37}$$

where F_s and F_d are the static and dynamic friction coefficients respectively. The friction coefficients are experimentally determined to be $F_s = 1{\cdot}05$ N and $F_d = 15{\cdot}23$ N s/m. The best regulation results are achieved with $k = 3{\cdot}0$ and $k_r = 3{\cdot}12$. Figure 6 shows the angular deflection $u_x(L, t)$, the gantry displacement $u(L, t)$, the time-varying tension signal $T(t)$, and the control voltage resulting from the initial displacement. The non-linear control response is only slightly improved compared to the linear control. Finally, the adaptive controller defined by equation (28) and the update laws given by equation (29) are implemented. The parameter estimates are initialized to 25% of their nominal values. The best regulation results are achieved with $k = 3{\cdot}0$, $k_r = 2{\cdot}97$, and $\Gamma = \text{diag}\{2{\cdot}55, 50, 0{\cdot}69\}$. Again, the response

[§]The sign function sgn(x) is defined as follows:

$$\text{sgn}(x) = \begin{cases} 1 & \text{if } x > 0, \\ 0 & \text{if } x = 0, \\ -1 & \text{if } x < 0. \end{cases}$$

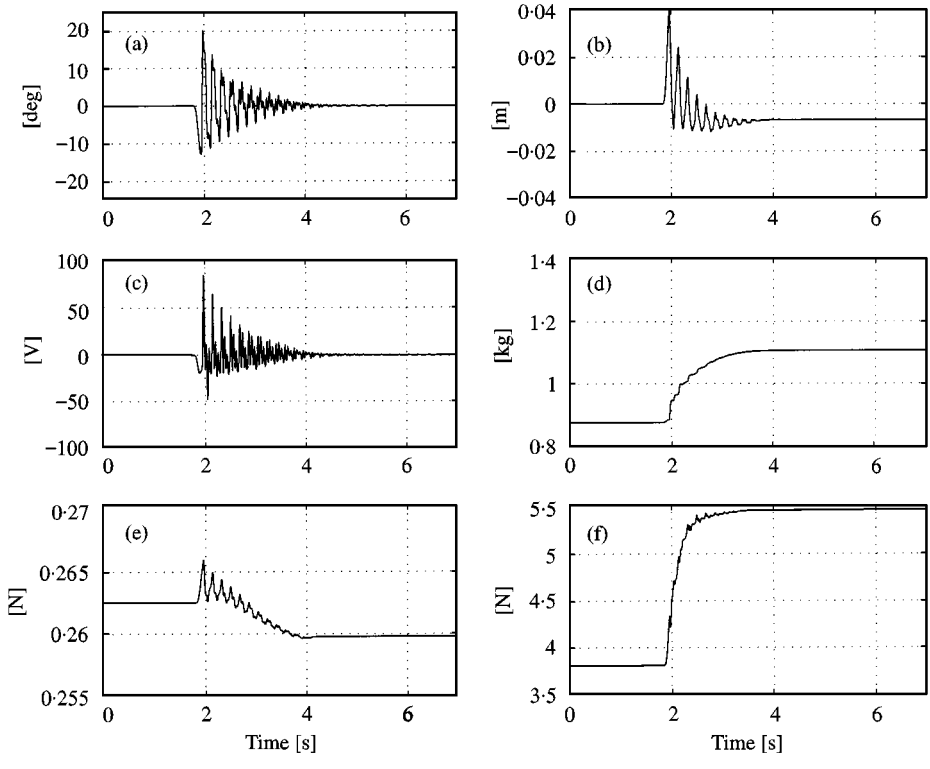

Figure 7. Experimental results for adaptive controller: (a) string deflection angle $u_x(L, t)$, (b) gantry displacement $u(L, t)$, (c) control voltage, (d) mass estimate $\hat{m}(t)$, (e) static friction coefficient estimate $\hat{F}_s(t)$, and (f) dynamic friction coefficient estimate $\hat{F}_d(t)$.

TABLE 1

Controller performance summary

Controller type	r.m.s. $u_x(L, t)$ (deg)	r.m.s. control voltage (V)
Open-loop system	2·75	—
Damper controller	1·98	4·91
Linear controller	1·94	6·25
Model-based controller	1·70	7·30
Adaptive controller	1·77	5·32

is similar to the previous two controllers. The estimated parameters converge to final values but not their exact values. Persistent excitation via sinusoidal or repeated impulse inputs would move the estimates to their actual values.

Table 1 compares the experimental performance of the controllers by computing the r.m.s. string deflection angle over a 10 s time interval. The trends in the r.m.s. data mirror the settling time performance, showing that the adaptive controller provides a 12% improvement in performance with similar control effort as compared to damper control.

5. CONCLUSION

In this paper, we design a class of boundary controllers that asymptotically drives the total energy of a non-linear string–actuator system to zero. The non-linear model relaxes the restrictive assumptions of previous work by including large amplitude displacements and the mass and non-linearities associated with the actuator. Experimental results demonstrate the implementability of the proposed control and the improved performance compared to damper or linear controllers.

ACKNOWLEDGMENT

This work is supported in part by the U.S. National Science Foundation Grants DMI-9457967, CMS-9634796, ECS-9619785, DOE Grant DE-FG07-96ER14728, the Square D Corporation, and the Union Camp Corporation.

REFERENCES

1. Z. Luo, N. Kitamura and B. Guo 1995 *IEEE Transactions on Robotics and Automation* **11**, 760–765. Shear force feedback control of flexible robot arms.
2. O. Morgül 1991 *IEEE Transactions on Automatic Control* **36**, 953–962. Orientation and stabilization of a flexible beam attached to a rigid body: planar motion.
3. C. Xu and J. Baillieul 1993 *IEEE Transactions on Automatic Control* **38**, 1754–1765. Stabilizability and stabilization of rotating body-beam system with torque control.
4. G. Sallet, C. Xu and H. Laousy 1995 *Proceedings of the IEEE Conference Decision and Control*, 930–935. Boundary feedback stabilization of a rotating body-beam system.
5. C. Baicu, C. Rahn and B. Nibali 1996 *Journal of Sound and Vibration* **198**, 17–26. Active boundary control of elastic cables: theory and experiment.
6. O. Morgül 1994 *Automatica* **30**, 1785–1792. A dynamic control law for the wave equation.
7. J. Shahruz and L. Krishna 1996 *Journal of Sound and Vibration* **195**, 169–174. Boundary control of a nonlinear string.
8. H. Canbolat, D. Dawson, C. Rahn and S. Nagarkatti 1997 *Proceedings of the American Control Conference*, 3547–3551. Boundary control of a flexible cable with actuator dynamics.
9. M. De Queiroz, D. Dawson, C. Rahn and F. Zhang *ASME Journal of Vibration and Acoustics*. Adaptive vibration control of an axially moving string (to appear).
10. S. Shahruz 1997 *Proceedings of the American Control Conference* 3242–3243. Supression of vibration in a nonlinear axially moving string by the boundary control.
11. D. Oplinger 1960 *Journal of the Acoustical Society of America* **32**, 1529–1538. Frequency response of a nonlinear stretched string.
12. G. Carrier 1945 *Quarterly of Applied Mathematics* **3**, 157–165. On the non-linear vibration problem of the elastic string.
13. J. Slotine and W. Li 1991 *Applied Nonlinear Control*. Englewood Cliff, NJ: Prentice Hall.
14. H. Canbolat, D. Dawson, C. Rahn and P. Vedagarbha 1997 *Proceedings of the ASME Adaptive Structures Forum*, 1589–1598. Boundary control of a cantilevered flexible beam with point-mass dynamics at the free end.
15. G. Hardy, J. Littlewood and G. Polya 1959 *Inequalities*. Cambridge: Cambridge University Press.
16. L. Meirovitch 1980 *Computational Methods in Structural Dynamics*. Rockvile, MD: Sijthoff & Noordhoff International Publishers B.V., Alphen aan den Rijn, The Netherlands.

17. A. Taylor 1985 *General Theory of Functions and Integration*. New York, NY: Dover Publications.

APPENDIX A: STABILITY LEMMAS

Lemma 1. *The time derivative of the function* $V_1(t)$ *defined in equation* (16) *can be upper bounded as* $\dot{V}_1(t) \leqslant 0$.

Proof. After differentiating equation (16) with respect to time, we obtain

$$\dot{V}_1 = \dot{E} - \left(k + \frac{k_r}{2} T(\cdot)\right)\eta^2, \tag{A1}$$

where equation (15) has been utilized. To obtain the expression for $\dot{E}(t)$ in equation (A1), we differentiate equation (17) with respect to time, and then substitute the field dynamics given by equation (7) and utilize the structure of $y(t)$ given in equation (4) to obtain

$$\dot{E} = T(\cdot)\left[\int_0^L u_t \frac{\partial}{\partial x}\left(\frac{u_x}{\sqrt{1+(u_x)^2}}\right)\mathrm{d}x\right] + T(\cdot)\int_0^L \frac{u_{xt}u_x}{\sqrt{1+(u_x)^2}}\,\mathrm{d}x. \tag{A2}$$

After integrating the bracketed term in equation (A2) by parts and cancelling common terms, we obtain

$$\dot{E} = T(\cdot)u_t(L)\frac{u_x(L)}{\sqrt{1+(u_x(L))^2}}, \tag{A3}$$

where the boundary condition given by equation (8) has been employed. We now rewrite equation (A3) in the advantageous form

$$\dot{E} = \frac{T(\cdot)}{2}\eta^2 - \frac{T(\cdot)}{2}\left(u_t^2(L) + \frac{u_x^2(L)}{1+u_x^2(L)}\right) \tag{A4}$$

by using the definition of $\eta(t)$ in equation (12). After substituting equation (A4) into equation (A1) and collecting common terms, we obtain

$$\dot{V}_1 = -\left(k + \frac{(k_r-1)}{2} T(\cdot)\right)\eta^2 - \frac{T(\cdot)}{2}\left(u_t(L) + \frac{u_x^2(L)}{1+u_x^2(L)}\right). \tag{A5}$$

Since k and k_r have been restricted according to equation (13), and $T(\cdot)$ is positive according to equation (2), we can see from equation (A5) that $\dot{V}_1(t)$ can be upper bounded as $\dot{V}_1(t) \leqslant 0$. □

Lemma 2. *The function* $V(t)$ *defined in equation* (19) *can be bounded as given by equation* (21), *where the positive constants* λ_1 *and* λ_2 *are defined by*

$$\lambda_1 = \min\left\{\left(\frac{1}{2} - \beta L\right), (\alpha_l - 2\beta\rho L\delta), \frac{m}{2}\right\}, \quad \lambda_2 = \max\left\{2\left(\frac{1}{2} + \beta L\right), 2\left(1 + 2\frac{\beta\rho L\delta}{\alpha_l}\right), \frac{m}{2}\right\}, \tag{A6}$$

where the weighting constant β must be selected to satisfy the following condition:

$$\beta < \min\left\{\frac{1}{2L}, \frac{\alpha_l}{2\rho L\delta}\right\} \tag{A7}$$

and δ is a positive bounding constant defined as

$$\delta \triangleq 1 + \sup_{x,t}\{(u_x(x,t))^2\}. \tag{A8}$$

Note, as illustrated by Lemma 1 and the first part of the proof of Theorem 1, we know that $u_x(x, t)$ is bounded for all $(x, t) \in [0, L] \times [0, \infty)$; hence, we know that the constant δ defined in equations (A8) exists.

Proof. To prove the above result, we first show that the summation of $E(t)$ and $E_c(t)$, defined in equations (17) and (20), respectively, can be bounded by

$$0 \leqslant \mu_1 E_a \leqslant E + E_c \leqslant 2\mu_2 E, \tag{A9}$$

where $E_a(t)$ is defined in equation (22), and μ_1, μ_2 are positive constants defined as

$$\mu_1 = \min\left\{\left(\frac{1}{2} - \beta L\right), (\alpha_l - 2\beta\rho L\delta)\right\} \quad \text{and} \quad \mu_2 = \max\left\{\left(\frac{1}{2} + \beta L\right), \left(1 + 2\frac{\beta\rho L\delta}{\alpha_l}\right)\right. \tag{A.10}$$

To prove the inequality given by equation (A9), we first note from equation (20) that

$$\begin{aligned} E_c &\leqslant 2\beta\rho \int_0^L x|u_t u_x|\,\mathrm{d}x \leqslant 2\beta\rho L \int_0^L |u_t||u_x|\,\mathrm{d}x \\ &\leqslant \beta\rho L\left(\int_0^L (u_t)^2\,\mathrm{d}x + \int_0^L (u_x)^2\,\mathrm{d}x\right). \end{aligned} \tag{A11}$$

After using equation (A8), we can utilize equation (A11) to form the following new upper bound for $E_c(t)$:

$$E_c \leqslant \beta\rho L \int_0^L (u_t)^2\,\mathrm{d}x + \beta\rho L\delta \int_0^L \left(\frac{u_x}{\sqrt{1 + (u_x)^2}}\right)^2 \mathrm{d}x. \tag{A12}$$

We can use the same procedure use to form the upper bound for $E_c(t)$ given in equation (A12) to formulate the following lower bound on $E_c(t)$:

$$-\beta\rho L \int_0^L (u_t)^2\,\mathrm{d}x - \beta\rho L\delta \int_0^L \left(\frac{u_x}{\sqrt{1 + (u_x)^2}}\right)^2 \mathrm{d}x \leqslant E_c. \tag{A13}$$

We now use equations (A13) and (17) to formulate the lower bound,

$$\left(\frac{1}{2} - \beta L\right)\int_0^L \rho(u_t)^2\,\mathrm{d}x + \left[\int_0^y T(\cdot)\,\mathrm{d}y - \beta\rho L\delta \int_0^L \left(\frac{u_x}{\sqrt{1 + (u_x)^2}}\right)^2 \mathrm{d}x\right] \leqslant E_c + E. \tag{A14}$$

We now proceed to develop a lower bound for the bracketed term in equation (A14). First, we note that it is easy to show that

$$\left(\frac{u_x}{\sqrt{1+(u_x)^2}}\right)^2 \leqslant 2(-1+\sqrt{1+(u_x)^2}). \tag{A15}$$

After multiplying both sides of equation (A15) by $-\beta\rho L\delta$ and then adding $\alpha_l(-1+\sqrt{1+(u_x)^2})$ to both sides of the resulting expression, we have

$$(\alpha_l - 2\beta\rho L\delta)(-1+\sqrt{1+(u_x)^2}) \leqslant -\beta\rho L\delta\frac{u_x}{1+(u_x)^2} + \alpha_l(-1+\sqrt{1+(u_x)^2}). \tag{A16}$$

Thus, if we restrict the weighting constant β according to

$$\beta < \frac{\alpha_l}{2\rho L\delta} \tag{A17}$$

as given in equation (A7), then the left-hand side of equation (A16) will always be non-negative. After integrating both sides of equation (A16), we obtain the inequality

$$0 \leqslant (\alpha_l - 2\beta\rho L\delta)\, y \leqslant -\beta\rho L\delta\int_0^L \left(\frac{u_x}{\sqrt{1+(u_x)^2}}\right)^2 \mathrm{d}x + \alpha_l y, \tag{A18}$$

where $y(t)$ was defined in equation (4). After using equation (3) to the right-hand side of equation (A18), we can formulate the inequality

$$0 \leqslant (\alpha_l - 2\beta\rho L\delta)\, y \leqslant -\beta\rho L\delta\int_0^L \left(\frac{u_x}{\sqrt{1+(u_x)^2}}\right)^2 \mathrm{d}x + \int_0^y T(\cdot)\,\mathrm{d}y. \tag{A19}$$

By using the left-hand side of equation (A19) to lower bound the bracketed term in equation (A14), we can form the inequality

$$0 \leqslant \left[\left(\frac{1}{2}-\beta L\right)\int_0^L \rho(u_t)^2\,\mathrm{d}x\right] + (\alpha_l - 2\beta\rho L\delta)\, y \leqslant E_c + E, \tag{A20}$$

where we further restrict the weighting constant β according to

$$\beta < 1/2L \tag{A21}$$

as given in equation (A7). We can now use equation (A20) to formulate the lower bound

$$\mu_1 E_a \leqslant E + E_c, \tag{A22}$$

where μ_1, $E(t)$ and $E_a(t)$ were defined in equations (A10), (17) and (22) respectively.

To determine the upper bound given in equation (A9), we utilize equations (A12) and (17) to obtain the upper bound

$$E + E_c \leqslant \left(\frac{1}{2}+\beta L\right)\int_0^L \rho(u_t)^2\,\mathrm{d}x + \int_0^y T(\cdot)\,\mathrm{d}y + \beta\rho L\delta\int_0^L \left(\frac{u_x}{\sqrt{1+(u_x)^2}}\right)^2 \mathrm{d}x. \tag{A23}$$

Hence, we can utilize equations (A15), (3), (4), and (A23) to obtain the inequalities

$$E + E_c \leqslant \left(\frac{1}{2} + \beta L\right) \int_0^L \rho (u_t)^2 \, \mathrm{d}x + \int_0^y T(\cdot) \, \mathrm{d}y + 2\beta\rho L\delta \int_0^L (-1 + \sqrt{1 + (u_x)^2}) \, \mathrm{d}x$$

$$\leqslant \left(\frac{1}{2} + \beta L\right) \int_0^L \rho (u_t)^2 \, \mathrm{d}x + \left(1 + \frac{2\beta\rho L\delta}{\alpha_l}\right) \int_0^y T(\cdot) \, \mathrm{d}y$$

$$\leqslant \mu_2 \left(\int_0^L \rho (u_t)^2 \, \mathrm{d}x + \int_0^y T(\cdot) \, \mathrm{d}y \right) \leqslant 2\mu_2 E, \tag{A24}$$

where μ_2 was defined in equation (A10), and $E(t)$ was defined in equation (17). From equations (A12), (A10), and (A24), the result given in equation (21) is obvious. □

Lemma 3. *If the weighting constant* β *is restricted according to*

$$\beta < \min \left\{ \frac{T_0}{2\rho L}, \frac{1}{4L\sqrt{\delta}} \right\}, \tag{A25}$$

we can have an upper bound for the time derivative of $V(t)$ *of equation* (19) *as given by equation* (23), *where* δ *is defined in equation* (A8).

Proof. After differentiating equation (19) with respect to time, we obtain

$$\dot{V} = \dot{V}_1 + \dot{E}_c. \tag{A26}$$

From Lemma 1, we know that $\dot{V}_1(t)$ can be expressed as in equation (A5). To obtain the expression for $\dot{E}_c(t)$ in equation (A26), we differentiate equation (20) respect to time as

$$\dot{E}_c(t) = A_1 + A_2, \tag{A27}$$

where the auxiliary variables $A_1(t)$ and $A_2(t)$ are given by

$$A_1 = 2\beta T(\cdot) \int_0^L x u_x \frac{\partial}{\partial x} \left(\frac{u_x}{\sqrt{1 + (u_x)^2}} \right) \mathrm{d}x, \quad A_2 = \beta\rho \int_0^L x \frac{\partial}{\partial x} ((u_t)^2) \, \mathrm{d}x \tag{A28}$$

and equation (7) has been utilized. After integrating $A_1(t)$ of equation (A28) by parts, we obtain the following expression for $A_1(t)$:

$$A_1 = 2\beta T(\cdot) L \frac{(u_x(L))^2}{\sqrt{1 + (u_x(L))^2}} - 2\beta T(\cdot) \int_0^L \frac{(u_x)^2}{\sqrt{1 + (u_x)^2}} \, \mathrm{d}x$$

$$- \left[2\beta T(\cdot) \int_0^L x \frac{\partial}{\partial x} (\sqrt{1 + (u_x)^2}) \, \mathrm{d}x \right], \tag{A29}$$

where the boundary conditions given by equation (8) have been employed. After integrating the bracketed term in equation (A29) by parts, we obtain the following expression for $A_1(t)$:

$$A = 2\beta T(\cdot)L\frac{(u_x(L))^2}{\sqrt{1+(u_x(L))^2}} - 2\beta T(\cdot)L(\sqrt{1+(u_x(L))^2}) \tag{A30}$$
$$- 2\beta T(\cdot)\int_0^L \left(\frac{(u_x)^2}{\sqrt{1+(u_x)^2}} - \sqrt{1+(u_x)^2}\right)\mathrm{d}x$$
$$+ \left[2\beta T(\cdot)L - 2\beta T(\cdot)\int_0^L 1\,\mathrm{d}x\right],$$

where the boundary conditions given by equation (8) have been employed, and the bracketed term that is equal to zero has been added to facilitate the analysis. After integrating $A_2(t)$ of equation (A28) by parts, the expression for $A_2(t)$ can be written as

$$A_2 = \beta\rho L(u_t(L))^2 - \beta\rho\int_0^L (u_t)^2\,\mathrm{d}x, \tag{A31}$$

where the boundary conditions given by equation (8) have been utilized.

We can now utilize equation (A27), (A30), and (A31) to write the expression for $\dot{E}_c(t)$ as

$$\dot{E}_c = 2\beta T(\cdot)L\frac{(u_x(L))^2}{\sqrt{1+(u_x(L))^2}} - 2\beta T(\cdot)L(-1+\sqrt{1+(u_x(L))^2}) + \beta\rho L u_t^2(L)$$
$$- \beta\rho\int_0^L (u_t)^2\,\mathrm{d}x - 2\beta T(\cdot)\int_0^L \left(\frac{(u_x)^2}{\sqrt{1+(u_x)^2}} + 1 - \sqrt{1+(u_x)^2}\right)\mathrm{d}x. \tag{A32}$$

After substituting equations (A32) and (A5) into equation (A26) and collecting collecting common terms, we obtain

$$\dot{V} = -\left(k + \frac{(k_r-1)}{2}T(\cdot)\right)\eta^2 - 2\beta T(\cdot)L(-1+\sqrt{1+(u_x(L))^2}) - \beta\rho\int_0^L (u_t)^2\,\mathrm{d}x$$
$$- \left(\frac{T(\cdot)}{2} - \beta\rho L\right)(u_t(L))^2 - \frac{T(\cdot)}{2}\left(\frac{1}{\sqrt{1+(u_x(L))^2}} - 4\beta L\right)\frac{(u_x(L))^2}{\sqrt{1+(u_x(L))^2}}$$
$$- 2\beta T(\cdot)\int_0^L \left(\frac{(u_x)^2}{\sqrt{1+(u_x)^2}} + 1 - \sqrt{1+(u_x)^2}\right)\mathrm{d}x. \tag{A33}$$

After applying equations (2), (13), (A8), and selecting β to satisfy equation (A25), we obtain the upper bound for $\dot{V}(t)$,

$$\dot{V} \leqslant -\kappa(u_t(L))^2 - \beta\rho\int_0^L (u_t)^2\,\mathrm{d}x - 2\beta T_0\int_0^L \left(\frac{(u_x)^2}{\sqrt{1+(u_x)^2}} + 1 - \sqrt{1+(u_x)^2}\right)\mathrm{d}x, \tag{A34}$$

where κ is some positive constant. Now, it is easy to show that

$$\frac{(u_x)^2}{\sqrt{1+(u_x)^2}} + 1 - \sqrt{1+(u_x)^2} \geqslant \frac{1}{2}\left(\frac{-1+\sqrt{1+(u_x)^2}}{\sqrt{1+(u_x)^2}}\right). \tag{A35}$$

After substituting equation (A35) into equation (A34) and using equation (A8), we can easily formulate the upper bound for $\dot{V}(t)$ as given in equation (23). □

Lemma 4. *If* (1) $V_a(t)$ *is a non-negative, scalar function that is lower bounded by zero* (2) $\dot{V}_a(t) \leqslant -f(t)$ *where* $f(t)$ *is a scalar, non-negative function, and* (3) $\dot{f}(t)$ *is bounded then*

$$\lim_{t\to\infty} f(t) = 0. \tag{A36}$$

Proof. First, we define the function

$$V_n(t) = V_a(t) - \int_0^t (\dot{V}_a(\tau) + f(\tau))\,\mathrm{d}\tau \tag{A37}$$

that is lower bounded by zero (since we have assumed that $V_a(t) \geqslant 0$ and that $\dot{V}_a(t) \leqslant -f(t)$, we know that $V_n(t) \geqslant 0$). If we differentiate equation (A37) with respect to time, we obtain

$$\dot{V}_n(t) = -f(t). \tag{A38}$$

We now apply a lemma from reference [13, p. 127] that states that if (1) $V_n(t)$ is a non-negative, scalar function that is lower bounded by zero, (2) $\dot{V}_n(t) = -f(t)$ where $f(t)$ is a scalar, non-negative function, and (3) $\dot{f}(t)$ is bounded then

$$\lim_{t\to\infty} f(t) = 0. \tag{A39}$$

Application of the above lemma to equations (A37) and (A38) yields the results given by equation (A36). □